

Analysis of the effect of seated posture on vertebral compression fractures in frontal crashes using HBMs

Taei Shibahara, Tetsuya Nishimoto, Tomokazu Motomura, Hisashi Matsumoto, Ryusuke Asahi, Shigeru Sugimoto, Masanobu Fukushima

Abstract Lumbar spine fractures have received increased attention recently, with anterior wedge and compression burst fractures the most commonly reported in frontal vehicle crashes. The objectives of this study are to analyse the effect of seated posture in frontal crashes by using THUMS ver.4.02. Referring to the compressive studies of whole and isolated vertebral column under dynamic loading conditions (Stemper *et al.* 2015 and 2018), material properties of the vertebral bodies and intervertebral discs in THUMS ver.4.02 were modified. A similar response was observed in the modified THUMS with the PMHS component tests under compressive loading conditions. -Spinal alignment in the seated posture can be broadly classified into kyphosis and S-shape. The stress on the vertebral body is higher when the spinal alignment of the occupant is kyphotic than when it is S-shaped. In order to reduce spinal injuries in frontal crashes, it is important to control the occupant's posture (spinal alignment).

Keywords Spine fractures, Thoracolumbar spine, Frontal crash, Spinal alignment, Anterior wedge fractures.

I. INTRODUCTION

Recently, the passive safety performance of automobiles has been improved with the strengthening of crash test regulations and New Car Assessment Programme (NCAP), which results in a significant decrease of head and chest injuries in frontal crashes. On the other hand, thoracolumbar spine injuries have a tendency to increase for occupants wearing seatbelts [1-2]. Additionally, a reclined seating posture, free from current restraint systems, is expected in highly automated vehicles of the future. It has been pointed out that serious injuries of the abdomen or thoracolumbar spine may occur due to a decrease of the seatbelt restraining force in a reclined posture [3]. As a result, thoracolumbar spine injuries are receiving particular attention.

Many thoracolumbar spine injuries occur predominantly from T12 to L5, particularly near the junction of the thoracic and lumbar spine [4-7]. The main contributors to thoracolumbar fractures are seat pan vertical stiffness and crash pulse [2][8]. In terms of fracture morphology, fractures can be classified into anterior wedge fractures, namely the partial crushing of frontal vertebral body, and compression burst fractures, namely the crushing of the whole vertebral body. The former occurs mainly by flexion, while the latter results from vertical loading [9-10].

In order to reduce fatalities or serious injuries in real-world scenarios, Mazda has collaborated in studies with the Nihon University College of Engineering and Nippon Medical School Chiba Hokusoh Hospital Shock and Trauma Centre since 2014. And since 2009 the Faculty of Engineering at Nihon University and the Shock and Trauma Centre of Nippon Medical School Chiba Hokusoh Hospital have been conducting accident investigations on patients transported to the Emergency and Critical Care Centre for traffic trauma. Medical and engineering teams have been working together to analyse the medical data of the accident vehicles and patients in order to identify the causes of accidents and the injury mechanisms. According to the 470 in-depth accident investigation data analyzed to date, 39 thoracolumbar compression fractures were extracted from the results of narrowing the cases with horizontal frontal crash, wearing a belt, and no multiple collisions. 30 cases of the thoracolumbar spine fractures occurred from T 12 to L5, of which 77% were anterior wedge fractures, and 23% compression burst fractures.

T. Shibahara (e-mail: shibahara.t@mazda.co.jp; tel: +81-82-287-5421) is an Assistant Manager, R. Asahi is a Technical Leader, S. Sugimoto is a Manager, Crash Safety Technology Development Group, and M. Fukushima is General Manager, Crash Safety Development Dept., all at Vehicle Development Div., Mazda Motor Corporation, Japan. T. Nishimoto is a Professor, Biomechanics Research Unit, College of Engineering, Nihon University, Japan. T. Motomura is a Clinical Assistant Professor, H. Matsumoto is a Professor, Shock and Trauma Centre, Nippon Medical School, Chiba Hokusoh Hospital, Japan.

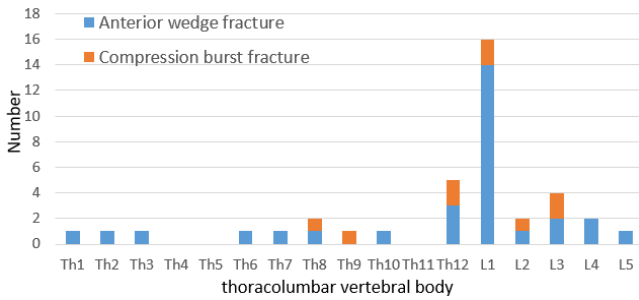


Fig. 1. Relationship between fracture type and thoracolumbar vertebral body.

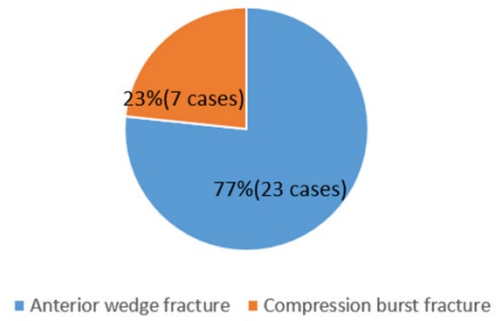


Fig. 2. Percentage of classification by vertebral fracture type N=30.

Past studies have indicated the rate of injury incidence by crash type using road traffic accident data, statistical percentage of spine injury incidence by age, sex and body size [11], vertebral body collapse characteristics on a specimen test basis [12], and local injury mechanism estimation [13-18]. However, few studies have been focused on the correlation between thoracolumbar compression fractures and occupant seating postures in frontal crashes.

In this study, the relationship between occupant seating postures and thoracolumbar compression fractures in frontal crashes was analysed using THUMS Ver4.02 with modified thoracolumbar vertebral body and intervertebral disc material properties.

II. METHODS

Modification of vertebral body and intervertebral disc material properties in human body model

Human body model THUMS ver.4.02, developed by Toyota Motor Corporation and Toyota Central R&D Labs., was used in this study. In THUMS ver.4.02, the skeleton and internal organs are modeled in detail based on CT scanning data, and the material properties of each part are defined to reproduce the cadaver response by referring literatures [19]. However, in order to apply THUMS to a detailed lumbar spine injury study, the material properties of both vertebral bodies and intervertebral discs are required to be validated with a dynamic loading condition at the level of compression rate observed in car crashes [16-17]. Dynamic compression tests were performed using Finite Element Method (FEM) analysis and parameters defined for material properties were modified to satisfy the fracture corridor.

Estimation of vertebral body collapse characteristics

For the analysis to reproduce the vertebral body compression test, L2 was extracted from THUMS Ver. 4.02 AM50, the transverse process and other parts of the posterior vertebral body were cut out, and the vertebral body alone was compressed at a compression rate of 0.6 m/s (Lower Rate) and 2.5 m/s (Higher Rate) [16]. Due to the difference of the vertebral body size between the specimen and THUMS, the compression results cannot be directly compared. Therefore, the vertebral body in THUMS were scaled to the size of that in compression test. The average cross-sectional area of the tested vertebral body was derived by dividing the peak force in the test by the fracture stress, and the average height of the tested vertebral body was derived by dividing the failure displacement by the fracture strain.

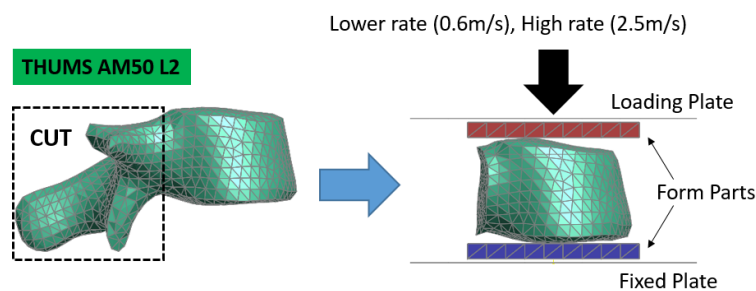


Fig. 3. The FE simulation model of THUMS L2 dynamic compression.

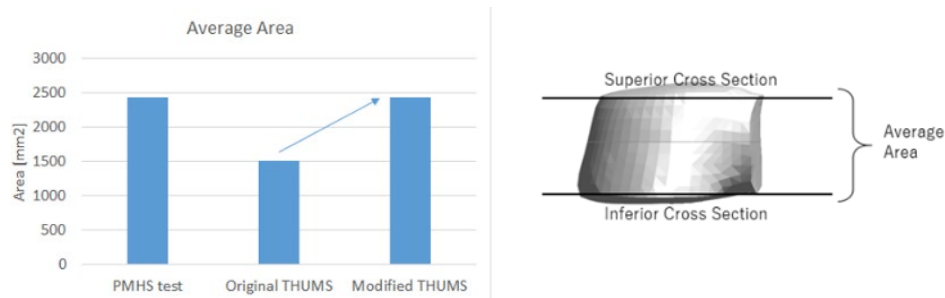


Fig. 4. Modification of vertebral cross-section.

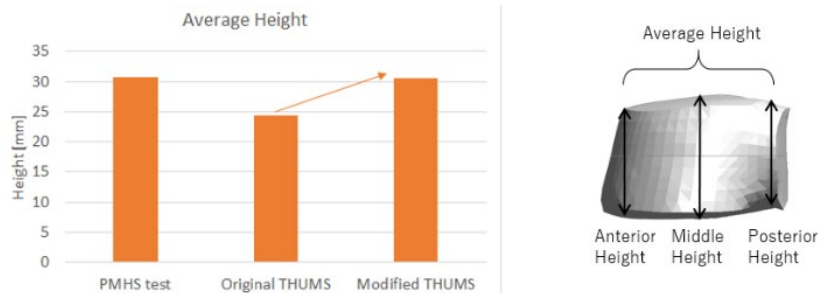


Fig. 5. Modification of vertebral cross-section.

Estimation of intervertebral disc dynamic collapse characteristics

In order to evaluate the intervertebral disc characteristics of THUMS with modified vertebral body material property, the dynamic component tests performed in [17] were selected from the previously performed lumbar component tests. In [17], the lumbar spine was rigidly potted in poly methyl methacrylate (PMMA) at the sacrum and T12 so that the intervertebral disc between L 2 and L 3 was horizontal. In order to prevent buckling during dynamic loading and to achieve a reliable compression along the spine axis, a 5Nm flexion was performed to produce a straight spine shape and compression tests were conducted with the load axis slightly forward of the spine centre. In this study, referring the testing procedure in [17], the thoracolumbar vertebrae from T12-L5 the L2-L3 plane was set vertically to the loading direction. A mass of 32 kg was loaded from the top, and the lower surface was covered with 15 times expanded polypropylene (EPP) foam to reproduce the G-levels measured in the test.

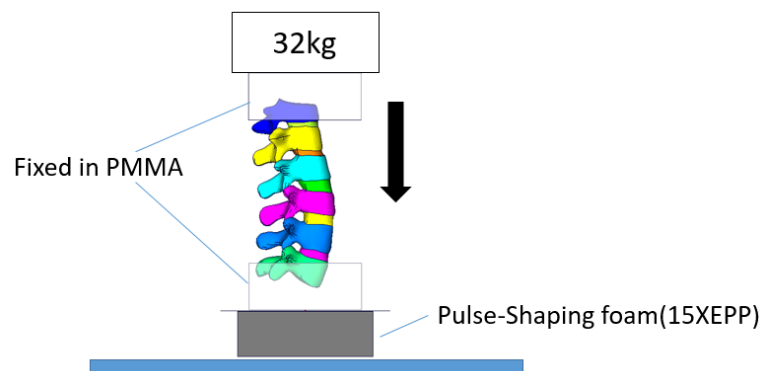


Fig. 6. The FE simulation model of T1-L5 dynamic compression. The top and bottom of the T12-L5 are fixed, and a mass of 32 kg is placed above and dropped.

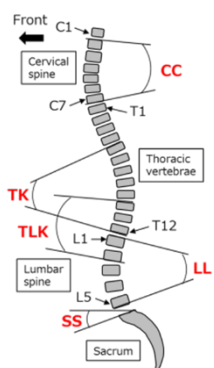
Preparation of the analysis model

Seated posture was analysed and selected for this study by referring to [20]. This study has provided X-ray photography data of 111 asymptomatic subjects sitting on an actual automotive seat. The data were obtained in an unbiased way with respect to age, sex and body size in order to reproduce the market situation in the real world.

Five parameters representing alignment of the spine were measured: CC, TK, TLK, LL and SS. This study focused specifically on the lumbar spine and pelvis in order to identify differences in the kinematics of the pelvic area due to the shape of the spine. Therefore, we analysed in detail the variation of LL according to gender, age, height and BMI.

In order to statistically infer the population, a normal distribution curve was applied to the data obtained from the X-rays. Representative LL distributions of the 90th percentile, 50th percentile, and 10th percentile were

then selected. With reference to the lumbar, sacral and pelvic angles of the subjects whose pelvic angle and LL were close to the respective representative angles, the skeletal alignment of the THUMS ver.4.02 AM50 was modified by applying prescribed movements to the vertebrae of the spine.



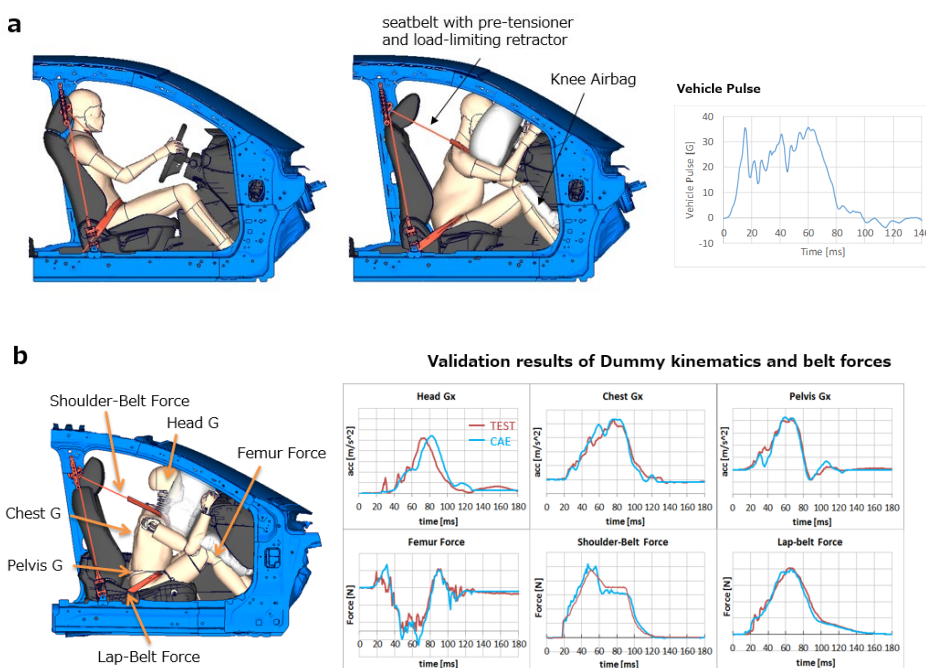
- Cervical curvature (CC): angle between C2 and C7
- Thoracic kyphosis (TK): angle between T5 and T12
- Thoracolumbar kyphosis (TLK): angle between T10 and L2
- Lumbar lordosis (LL): Angle between L1 and L5
- Sacral slope (SS): angle between the horizontal and the sacral plate

Fig. 7. Measurement items for spine.

FEM analysis conditions

In this study, simulations were conducted with the same condition of JNCAP 56kph full frontal crash to analyze the occupant kinematics in a frontal crash (Fig. 8a). Car models included in simulation were based on Mazda’s typical specification and the 6 DOF accelerations were applied to the car body about its CG in order to simulate the vehicle kinematics. The validation results of simulation model with the Hybrid III AM50 dummy were shown in Fig. 8b. The similar dummy kinematics and seatbelt forces in CAE simulation were confirmed by comparison to that in sled test. Besides, the validation results of THUMS ver.4 with NHTSA PMHS tests [21-22] were shown in Fig. 8c. The graph showed that the kinematics of the THUMS model was almost the same as that of the PMHS.

THUMS AM50 with modified vertebral body and intervertebral disc characteristics was used to investigate the occupant kinematics. These models were placed in the driver’s seat and restrained by seatbelts with pretensioners and load-limiting retractors. Frontal airbag and knee airbag models were installed to the steering part and the bottom of the instrument panel part. THUMS was positioned with hands on the wheel, while feet were on the accelerator pedal and footrest. The position and angle of the pelvis, spine and head depended on the corresponding arrangement. Shoulder and lap seatbelts were fitted to the chest and pelvis, respectively. The seat cushions were pre-deformed to account for initial compression by the gravity.



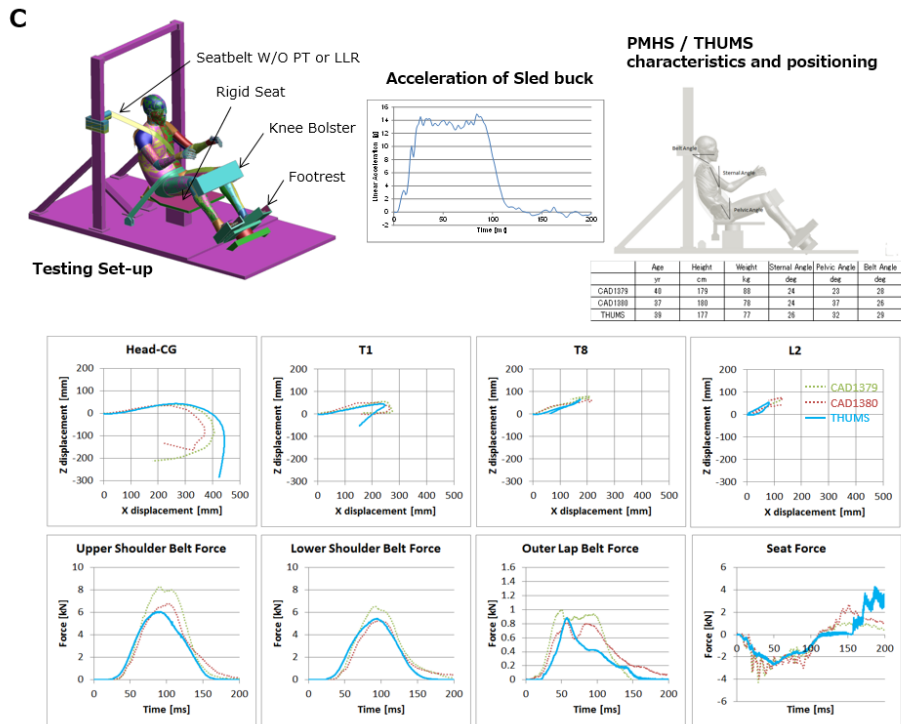


Fig. 8. a. The FE simulation model and the kinematics validation results of b. vehicle model and c. THUMS model

Analysis of Injury Measures

In order to clarify the mechanism of vertebral body compression fracture in a frontal crash and the effect of spinal alignment, the vertical load F_z and moment M_y acting on each vertebral body were analysed at the timing of maximum stress. Furthermore, injury values such as HIC15, F_z and M_y at C2, chest deflection at T4, acetabulum force, femur force were also measured.

III. RESULTS

From the results analysing the compression test of a single vertebral body defined the characteristics of Table I, it was indicated that both stress-strain curves at compression rates of 0.6 m/s (Lower Rate) and 2.5 m/s (Higher Rate) fell within the human corridors (Fig. 9). In other words, the improved vertebral body model could be applicable to local fractures regardless of vertebral body size.

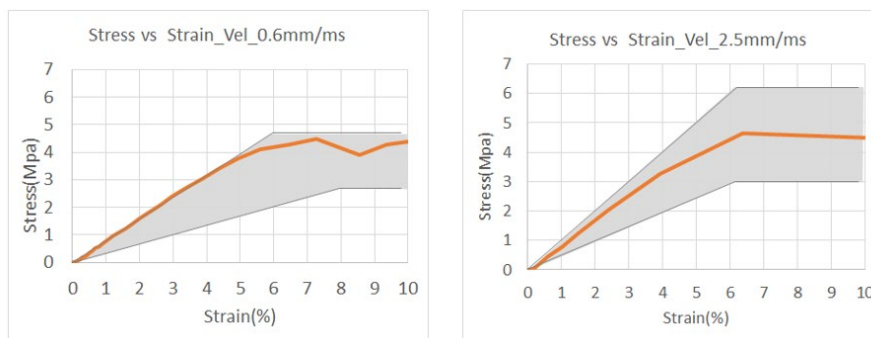


Fig. 9. The calibration results of vertebral body. Both the lower rate and the higher rate results fall within the human corridor represented by the hatch

T12 to L5, which is a straight shape, was generated by interweaving LL50 vertebral geometry and drop tests were conducted with a 32 kg mass load. As a result, it was confirmed that by defining the characteristics of vertebral bodies and intervertebral discs as defined in Table I, the corridors defined from the mean and standard deviation of the peak acceleration/compression force measured in [17], acceleration 28 ± 13 (G) and compression force 5.5 ± 1.2 (kN), were satisfied.

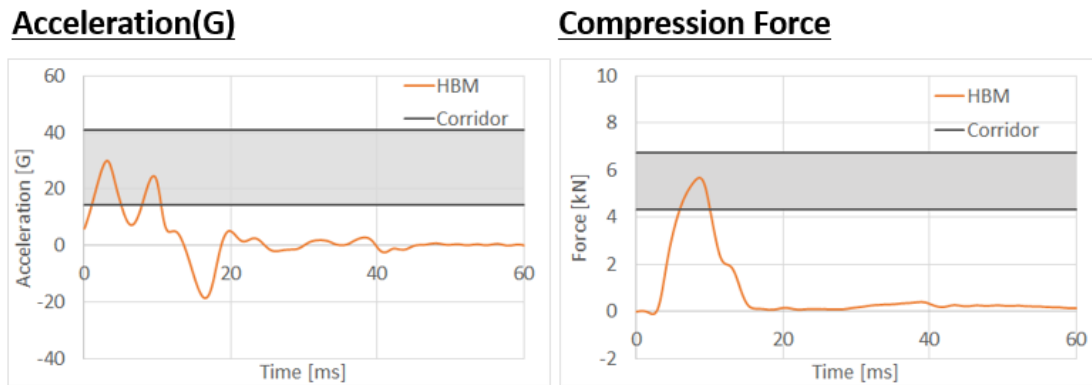


Fig. 10. The calibration results of acceleration and compression force in T12-L5 drop test.

As the detailed spinal geometries oriented with 5Nm flexion were not shown in [17], those geometries were generated from our X-ray data to account for individual differences in seated posture. On the basis of the measurement data, the cumulative distribution curve of LL and the number of subjects corresponding to each LL were drawn for all subjects in Fig. 10. In this figure, LL50 represented 0 degrees of lumbar lordosis, namely a straight alignment. On the other hand, LL90 represented +15 degrees (S-shaped), and LL10 was -14 degrees, representing kyphosis. The skeletal alignment of the THUMS was modified to LL90, LL50 and LL10.

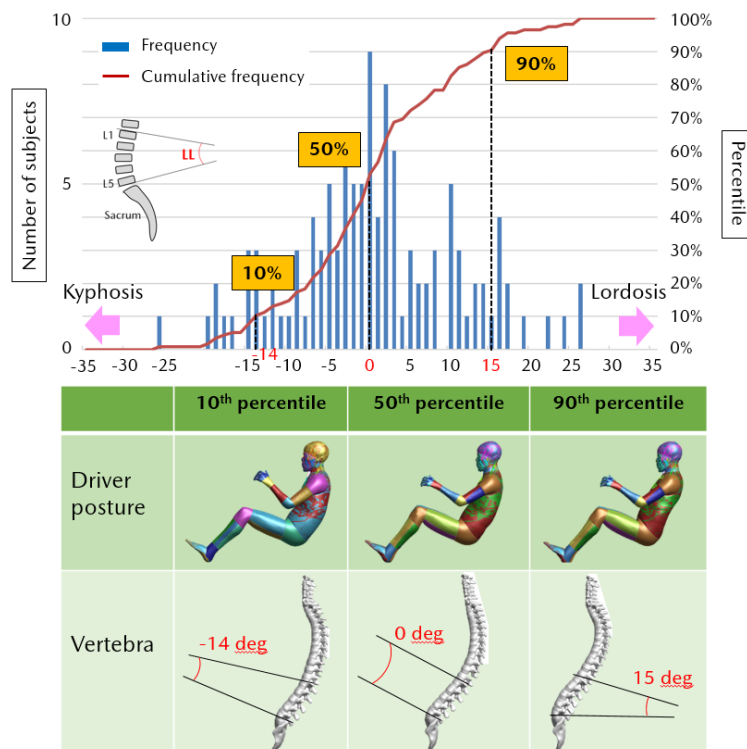


Fig. 11. Cumulative distribution of spinal alignment based on data of subjects.

TABLE I
 VERTEBRAL BODY AND INTERVERTEBRAL DISC MATERIAL DEFINITIONS USED IN THE MODIFIED THUMS

Component		Material Type & Parameters in LS-DYNA
Vertebral Body	Cortical Bone	*MAT_PLASTICITY_WITH_DAMAGE $\rho = 2.00E - 06 \frac{kg}{mm^3}$ $E = 23 \text{ GPa}$ $\sigma_y = 0.16 \text{ GPa}$ $\epsilon_{fail} = 0.02$
	Cancellous Bone	*MAT_DAMAGE2 $\rho = 1.00E - 06 \frac{kg}{mm^3}$ $E = 0.04 \text{ GPa}$ $\sigma_y = 0.0018 \text{ GPa}$
Intervertebral Disc	Nucleus Pulposus	*MAT_ISOTROPIC_ELASTIC_PLASTIC $\rho = 1.00E - 06 \frac{kg}{mm^3}$ $E = 4.33E-06 \text{ GPa}$ $\sigma_y = 1.30E-05 \text{ GPa}$
	Annulus Fibrosus	*MAT_FU_CHANG_FOAM $\rho = 1.00E - 06 \frac{kg}{mm^3}$ $E = 0.0021 \text{ GPa}$

Using the LL50 model, the loads and moments acting on the vertebrae was analysed at the timing of the maximum stress (0.18 Gpa) on L3 (Fig. 12). The results indicated that My acted on the vertebrae due to the flexion of the upper body and the vertical load Fz acted from the seat pan.

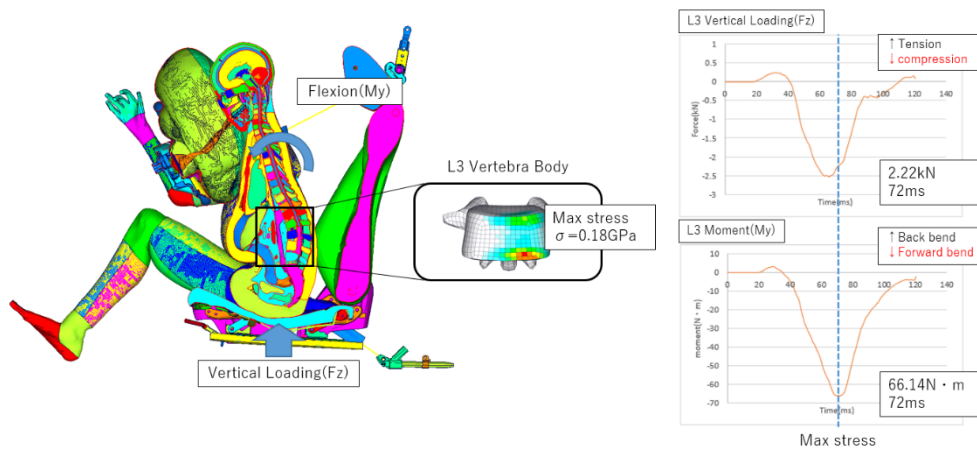


Fig. 12. The FE simulation of sled test: L3 vertical load (Fz) and L3 moment (My).

When the spinal alignment changed from kyphosis (LL10) to S-shape (LL90), the contribution of Fz and My acting on the vertebral body changed (Fig. 13). In kyphosis (LL10), the flexion bending moment of the spine increased and anterior wedge fractures occurred. On the other hand, when the spinal alignment changed from kyphosis (LL10) to S-shape (LL90), the stress output shifted to the posterior part of the vertebral body and the vertical force applied to the whole vertebral body increased, which may lead to the occurrence of compression burst fracture. In a frontal crash, however, the upper body of occupant bends forwards and anterior wedge fractures tend to occur more frequently, as shown in the accident analysis results (Fig. 2), regardless of spinal alignment.

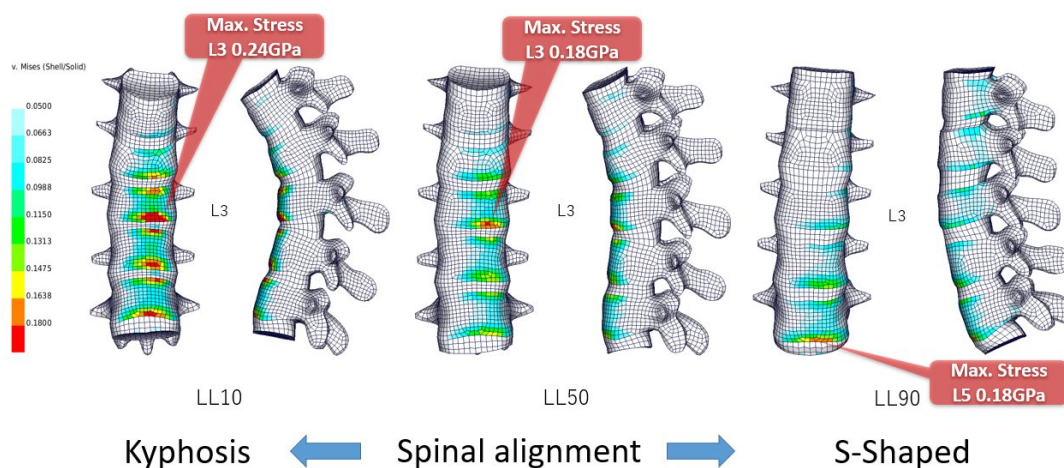


Fig. 13. Analysis of the stress distribution from lumbar kyphosis to lumbar lordosis.

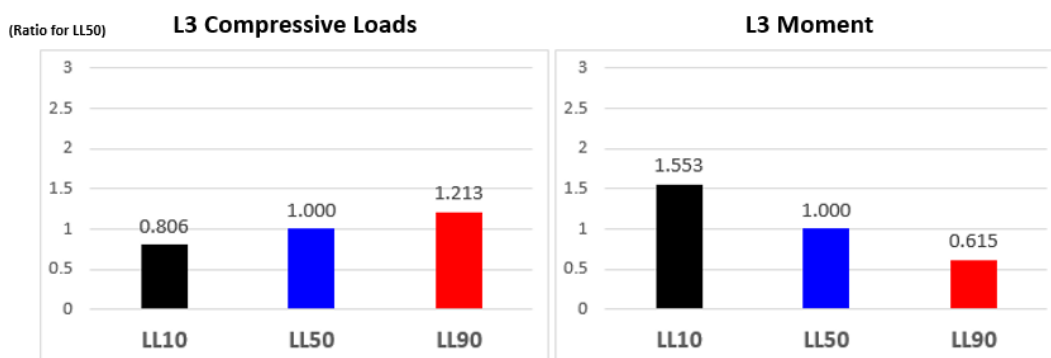


Fig. 14. Kinematics analysis of injury measurements around L3.

Furthermore, the effects on the kinematics of the other regions (head, neck, chest and thighs) were measured and there was little difference among three models for all injury values, such as HIC15, neck My, FZ and chest displacement, except for the femur load. Because the spinal alignment is more kyphotic and the pelvic angle is also greater, resulting in greater forward lumbar translation and higher femoral loading, the femur load in LL10 seems to be the highest among three models. The difference in C2 moment appears to be due to the low absolute values of less than 5 Nm in all cases (Fig. 15).

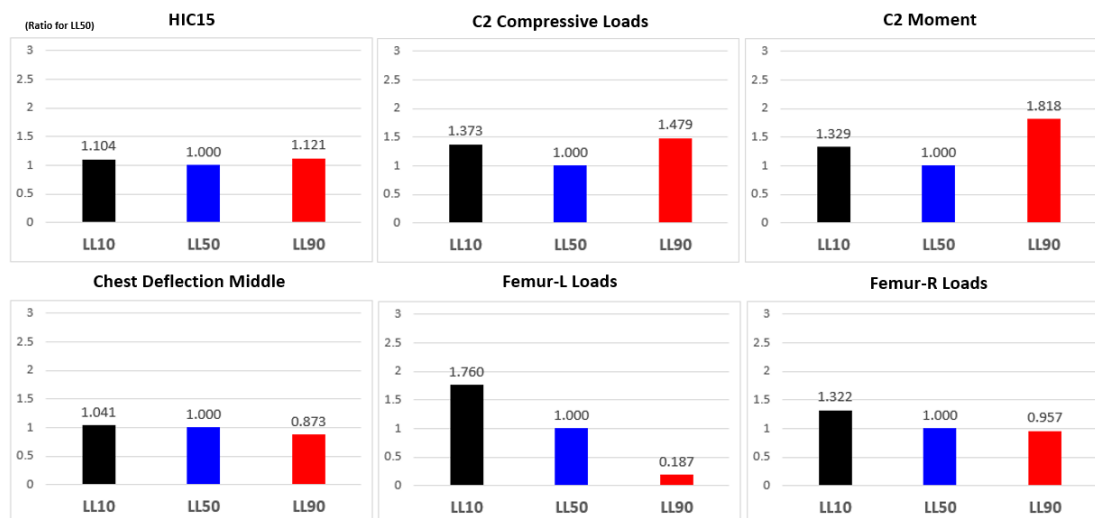


Fig. 15. Kinematics analysis of injury measurements for head, neck, chest and femur.

IV. DISCUSSION

The analysis of the results revealed that F_z of the LL50 model was 2.22 kN at the time of maximum stress on the L3 vertebral body and that the value was sufficiently smaller compared with the vertebral body's 50% injury risk value (95%CI), of 4.5 (3.9-5.2) kN. This suggests that the moment around the y-axis causing hyperflexion of the upper body is mainly responsible for vertebral body anterior wedge fracture.

If the spinal alignment is kyphotic ($-15^\circ \leq LL < 0^\circ$), the gap in front of the vertebral body is small and the upper body bends during a frontal crash, resulting in greater compression of the front of the vertebral body. If the vertebral alignment is S-shaped ($0^\circ < LL \leq 15^\circ$), the direction of vertical load and axial direction coincide and the whole vertebral body is compressed. In a frontal impact, the upper body flexes forwards and the contribution to vertebral compression fracture is considered to be flexion (M_y) > vertical loading (F_z). The stresses generated in the vertebral body are higher in the kyphosis type than in the S-shaped type.

Clinically, anterior wedge fractures with damage the front of the vertebral body due to the vertebral kyphotic alignment cause less spinal cord damage and less permanent disability than fractures, which crush the entire vertebral body due to the vertebral S-shaped alignment. However, submarine is more likely to occur in the spinal kyphotic alignment, therefore it is important to take both into account [23].

LIMITATIONS

In this study, to investigate the effect of differences of spinal alignment in seated posture on spinal compression fractures in frontal crashes, a model of the same size and flesh thickness was used with modified only the pelvic angle and spinal alignment. The crash condition was a horizontal frontal crash with a 3-point seatbelt, frontal airbag and knee airbag, and it should be noted that the simulation results may differ depending on the crash condition and belt position. In addition, although the stress/strain fracture data in this study were generated from the results of [17] considering only compression, this relationship may not be applicable in more complex conditions considering both flexion and compression.

V. CONCLUSIONS

- The biofidelity of the modified lumbar model was confirmed by calibrating the vertebral column and the whole lumbar spine in compression tests.
- The results of FE simulation show that vertebral compression fractures are caused by F_z acting on the vertebrae due to the reaction force from the seat, and the moment M_y acting around Y axis due to the upper body rotation behaviour of the occupant. In the case of a frontal crash, the stress generated in the vertebral body is highly correlated with M_y , and the contribution to spinal compression fracture is considered to be flexion (M_y) > vertical load (F_z).
- The stress on the vertebral body is higher when the spinal alignment of the occupant is kyphotic than when it is S-shaped. In order to reduce spinal injuries in frontal crashes, it is important to control the occupant's posture (spinal alignment).

VI. ACKNOWLEDGEMENTS

We would like to thank all staff and students in Nihon University and Nippon Medical School Chiba Hokusoh Hospital for providing great support in this project.

VII. REFERENCES

- [1] Kaufman, R. P., Ching, R. P. *et al.* (2013) Burst fracture of the lumbar spine in front crash. *Accident Analysis and Prevention*, 2013, **59**: pp.153–163.
- [2] Pintar, F. A., Yoganandan, N., Maiman, D. J. (2012) Thoracolumbar Spine Fractures in Frontal Impact Crashes. *Annals of Advances in Automotive Medicine*, **56**: pp.277–83.
- [3] Draper, D., Huf, A., Wernicke, P., Peldschus, S. (2019) The Influence of Reclined Seating Positions on Lumbar Spine Kinematics and Loading in Frontal Impact Scenarios. *Proceedings of the 26th ESV conference*, 2019, Eindhoven, Netherlands. Paper no. 19-0062.
- [4] Jakobsson, L., Bjorklund, M., Westerlund, L. (2016) Thoracolumbar spine Injuries in Car Crashes. *Proceedings of IRCOBI Conference*, 2016, Madrid.

- [5] Jakobsson, L., Bergman, T., Johansson, L. (2006) Identifying Thoracic and Lumbar Spinal Injuries in Car Accidents. *Proceedings of IRCOBI Conference*, 2006, Madrid.
- [6] Kurose, T., Kikuchi, A., Tominaga, S., Motomura, T., Nishimoto, T. (2018) Classification of spinal fractures for seat belt-restrained occupants in front impact. *Proceedings of 2018 JSAE Congress (Autumn)*, 2018, Nagoya (in Japanese).
- [7] Adolph, T., Wisch, M. *et al.* (2013) Analyses of Thoracic and Lumbar Spine Injuries in Frontal Impact. *Proceedings of IRCOBI Conference on Biomechanics of Impacts*, 2013, Gothenburg, Sweden.
- [8] Pintar, F. "Thoraco-Lumbar Spine fractures in Frontal Impacts". Internet:[<http://www.nhtsa.gov/DOT/NHTSA/NVS/CIREN/Presentations/2012/WiscCIREN%20Sept2012.pdf>], 2012 updated [accessed January 2015].
- [9] Ching, R., Kaufman, R., Mack, C., Bulger, E. "Vertebral Body Fractures of the L-spine in Frontal Crashes". Internet:[<http://www.nhtsa.gov/DOT/NHTSA/NVS/CIREN/2009%20Presentations/SeattleOct09.pdf>], 2009 updated [accessed January 2015].
- [10] Ejima, S., Kohoyda-Inglis, C., *et al.* (2018) Thoracolumbar Spine Fracture occurring in Obese People involved in Motor Vehicle Crashes. *Proceedings of IRCOBI Conference*, 2018, Athens (Greece).
- [11] Rao, R. D., Berry, C. A., *et al.* (2014) Occupant and Crash Characteristics in Thoracic and Lumbar Spine Injuries Resulting from Motor Vehicle Collisions. *The Spine Journal*, **14**(10): pp.2355–65.
- [12] Ochia, R. S., Tencer, A. F., Ching, R. P. (2003) Effect of Loading Rate on Endplate and Vertebral Body Strength in Human Lumbar Vertebrae. *Journal of Biomechanics*, **36**: pp.1875-1881.
- [13] Duma, S. M., Kemper, A. R., McNeely, D. M., Brolinson, P. G., Matsouka, F. (2006) Biomechanical Response Of the Lumbar Spine in Dynamic Compression. *Biomed Sci Instrum*, **42**: pp.476–81.
- [14] Kemper, A., McNally, C., Manoogian, S., Mcneely S., Duma, S. (2007) Stiffness Properties of Human Lumbar Intervertebral Discs in Compression and the Influence of Strain Rate. *Proceedings of the 20th ESV conference*, 2007, Lyon, France. Paper no. 07-0471.
- [15] Yoganandan, N., Arun, M. W. J., Stemper, B. D., Pintar, F. A., Maiman, D. J. (2013) Biomechanics of Human Thoracolumbar Spinal Column Trauma from Vertical Impact Loading. *Ann Adv Automot Med.*, **57**: pp.155–66.
- [16] Stemper, B. D., *et al.* (2015) Rate-Dependent Fracture Characteristics of Lumbar Vertebral Bodies. *Journal of the mechanical behavior of biomedical materials*, **41**: pp.271–279.
- [17] Stemper, B. D., *et al.* (2018) Biomechanical Tolerance of Whole Lumbar Spines in Straightened Posture Subjected to Axial Acceleration. *Journal of Orthopaedic Research*, **36**(6): pp.1746–1756.
- [18] Arun, M. W. J., Hadagali, P. *et al.* (2017) Biomechanics of Lumbar Motion-Segments in Dynamic Compression. *Stapp Car Crash Journal*, 2017, **61**: pp.1–25.
- [19] Toyota Motor Corporation. "About THUMS-Validations". Internet:[<https://www.toyota.co.jp/thums/about/>], 2021 updated [accessed June 2021].
- [20] Izumiyama, T., *et al.* (2018) The Analysis of an Individual Difference in Human Skeletal Alignment in Seated Posture and Occupant Behavior Using HBMs. *Proceedings of IRCOBI Conference*, 2018, Athens, Greece.
- [21] Crandall, J. "ATD Thoracic Response Test Development – THOR NT Advanced Frontal Crash Test Dummy, Frontal Sled Tests – UVA1379. *Center for Applied Biomechanics, Automobile Safety Laboratory, University of Virginia*. 2008. A Report Prepared for NHTSA, Cooperative Agreement No. DTNH22-93-Y-07028". Internet: [https://www.nrd.nhtsa.dot.gov/database/VSR/SearchMedia.aspx?database=b&tstno=11015&mediatype=r&r_tstno=11015], 2008 Updated [accessed June 2021].
- [22] Crandall, J. "ATD Thoracic Response Test Development – THOR NT Advanced Frontal Crash Test Dummy, Frontal Sled Tests – UVA1380. *Center for Applied Biomechanics, Automobile Safety Laboratory, University of Virginia*. 2013. A Report Prepared for NHTSA, Cooperative Agreement No. DTNH22-93-Y-07028". Internet: [https://www.nrd.nhtsa.dot.gov/database/VSR/SearchMedia.aspx?database=b&tstno=11016&mediatype=r&r_tstno=11016], 2008 Updated [accessed June 2021].
- [23] Langrana, N. A., Harten, R. D., Lin, D. C., Reiter, M. F., Lee, C. K. (2002) Acute Thoracolumbar Burst Fractures A New View of Loading Mechanisms. *Spine*, **27**(5): pp.498–508.